

The Integral-differential and Integral Approach for the Exact Solution of the Hybrid Functional Forms for Morse Potential

Surulere S. A., Shatalov M. Y., Mkolesia A. C., Malange T. N., and Adeniji A. A.

Abstract—The Morse potential, which is the most widely used potential in evaluating the vibrational energies of diatomic molecules, is studied and its unknown parameters were estimated in this paper. The integral-differential and integral approaches which are relatively more accurate approaches of the objective least squares function method were discussed and applied in this paper. The approaches were used to estimate the Classical and Generalized Morse potential parameters. The estimates obtained for the Classical Morse potential was used to obtain the Morse potential parameters.

The approaches were used to identify new unknown parameters of the Classical and Generalized Morse potential. They were also used to approximate parameters which were fundamental to graphically identifying the potentials using potential energy curves. The approach consists of recognizing the functional form of the hybrid forms of the Morse potential as the solution of some second order ordinary differential equation with unknown parameters. Then constructing the first objective function and integrating once (for the integral-differential method) and twice (for the integral method). The second objective function is constructed from the functional forms of the Classical and Generalized Morse potential under paper. A matrix system with the unknown parameters is formulated and numerical simulation of the system is done using gold atom experimental data sets.

The objective function values and reconstructed potential energy curves fitted to experimental data sets of gold atom shows high accuracy to the optimum solution when compared to the objective least squares function method. The estimated parameters approximates to the experimental data sets of gold atom through the range of interatomic distance.

Index Terms—least squares, interatomic potentials, parameter estimation, potential energy curves, differential equations.

I. INTRODUCTION

ENERGY potentials are widely considered to be of a great importance in computational chemistry. This is due to the fact that potential energy functions provide qualitative description of the energy-distance relationship

Manuscript received July 22, 2019; revised September 23, 2019. The authors thank and acknowledge the Department of Mathematics and Statistics and the Department of Higher Education and Training for funding this research.

Surulere S. A. is with the Department of Mathematics and Statistics, Faculty of Science, Tshwane University of Technology, Pretoria, 0081 ZA e-mail: samuel.abayomi.sas@gmail.com

Shatalov M. Y., Mkolesia A. C., Malange T. N. and Adeniji A. A. are with Department of Mathematics and Statistics, Faculty of Science, Tshwane University of Technology, Pretoria, 0081 ZA.

of the chemical bond [11]. The Morse potential, originally proposed by Philip Morse [7]

$$U_M = D[e^{-2\alpha(x-x_m)} - 2e^{-\alpha(x-x_m)}], \quad (1)$$

is used not only in molecular spectroscopy but also for the evaluation of kinetic properties of gases and in studies of crystal properties. The Morse potential has been and still is one of the most used and convenient model that provides an excellent, qualitative description of the interaction between two atoms in a diatomic molecule [1]. The Morse potential function, (or its hybrid forms) are used in many problems related to metallic systems [12] and it has been used frequently to paper the atomic and configuration properties of pure metals [2]. The hybrid functional forms of the Morse potential (which are the Classical and Generalized Morse potentials) are obtained through the expansion of Equation (1) and making relevant substitutions. After the expansion of Equation (1), we will use α_1 to represent the Classical Morse potential parameter and α_2, α_3 to represent the Generalized Morse potential parameters.

The hybrid forms of the Morse potential considered in this paper, are both nonlinear transcendental least squares problems. Several methods exist for estimating the parameters of nonlinear systems using approximations of a system of linear equations, since solving these systems can be an exhaustive task analytically [3]. Mathematical methods exist that permit standardization of the fitting procedure. The method of maximum likelihood and the least-square method are the most common [4]. Of these two methods, the least squares approach which requires initial guess values is more applied for solving transcendental problems [6]. In this paper, we introduce more efficient approaches for identifying the parameters of the Morse potential which guarantees better approximations than results obtained from previous studies [16] as well as in the literature. We also concisely introduce an alternative novel approach for identifying the energy potentials and make a comparison of both methods. The aim of this paper is validated through the construction and reconstruction of potential energy curves (PECs) and the values of objective function presented in Table I. The paper also reveals that the Classical Morse potential is not a stable hybrid functional form of the Morse potential as compared to the Generalized Morse potential.

This paper is structured as follows: Section II introduces

the integral-differential and integral approaches to be applied in this paper, In Section III-A, the integral-differential method is used to estimate parameters of the Classical Morse potential while the parameters of the Generalized Morse potential are estimated in Section III-C. Section IV-A discusses the approach of the integral method for estimation of the Classical Morse potential, Section IV-B estimates parameters of the Generalized Morse potential using the integral method. Section V concisely presents an alternative approach for identifying the energy potentials, the obtained research results are discussed and summarized in Section VI and conclusion of the paper is presented in Section VII.

II. MATERIALS AND METHODS

The Objective least squares function method (ObLSf) with differential, integral-differential and integral approaches were first discussed in [3] (where it was referred to as the multiple goal function, MGF method). In [6], the MGF method with the three aforementioned approaches were used to identify the Classical Rydberg potential energy function using experimental data sets of Copper, Silver and Copper-Silver alloy. The author(s) in [16] coined the ObLSf term and used it (with the differential approach alone) to identify the Classical and Generalized Morse potential function using experimental data sets of gold atom. The integral-differential and integral approach consists of constructing two objective functions. The first one is constructed from the functional form of the Classical and Generalized Morse potential which is considered to be the solution to some second order ordinary differential equation. The second objective function is constructed from the functional form of the Classical and Generalized Morse potential functional form. Each of the objective functions is partially differentiated with respect to the unknown parameters and a matrix system is formulated. This matrix system with the unknowns is numerically simulated to yield estimates for the parameters. The unknown parameter estimates obtained using the first objective function is used to obtain the unknown parameters of the Classical and Generalized Morse potential. The unknown parameters of the mentioned energy potentials are obtained from the constructed second objective function.

Traditional approaches of estimating parameters of transcendental equations such as Levenberg-Marquardt, Gauss-Newton, Powell Dog Leg, Maximum Likelihood [8] all require the provision of initial guess values of which convergence to optimal solution is not always guaranteed. The methods discussed in this paper overcomes the setbacks and limitations of previous well-known approaches of solving nonlinear transcendental least squares problems and also produced more accurate results than was obtained in recent studies [16]. This paper applies both the integral-differential and integral methods to estimate parameters of the Classical and Generalized Morse potential. The approaches both involves numerical integration (once and twice respectively) of the second order ODE, construction of the first objective function to estimate parameter(s) α_1 for the Classical Morse potential and α_2, α_3 for the Generalized Morse potential. The

formulated matrix system is numerically simulated in MathCad[®] to obtain numerical approximations which are used to construct the second objective function and estimate the parameters A_{CM}, B_{CM} and A_{GM} and B_{GM} . Several authors have applied the MGF method to solving various nonlinear transcendental problems. [14] used the ObLSf method for estimation of the Rayleigh distribution parameter. [5] also used the ObLSf method for parameter estimation of different probability density functions. The ObLSf method was used in [9] to identify parameters of epidemiological models under missing observable data.

III. INTEGRAL-DIFFERENTIAL METHOD TO ESTIMATE PARAMETERS OF THE HYBRID FORMS OF MORSE POTENTIAL

The integral-differential approach requires taking the first integral of the second-order ODE with the boundaries $[r_o, r]$. We now estimate the parameters of the Classical and Generalized Morse potentials in the next sections.

A. Classical Morse potential energy function

The functional form of the Classical Morse potential is

$$U_{CM} = A_{CM}e^{-2\alpha_1 r} - B_{CM}e^{-\alpha_1 r}. \quad (2)$$

From the knowledge of ordinary differential equations (ODE), Equation (2) is the solution of some second-order linear homogeneous ODE

$$\frac{d^2U}{dr^2} + (2\alpha_1 + \alpha_1) \frac{dU}{dr} + (2\alpha_1 \cdot \alpha_1)U = 0. \quad (3)$$

Equation (3) is written as

$$\frac{d^2U}{dr^2} + a_1 \frac{dU}{dr} + a_2U = 0, \quad (4)$$

where a_1 and a_2 are new unknown parameters. The constraint equation of Equation (3) is written as $g[a_1(\lambda), a_2(\lambda)] = [2a_1(\lambda)]^2 - 9[a_2(\lambda)]$. Integrating Equation (4) with respect to r on the integral domain $[r_0, r]$ to obtain

$$\frac{dU}{dr} + a_1U + a_2 \int_{r_0}^r U(\rho)d\rho + c_1 = 0, \quad (5)$$

where we introduced c_1 to replace $\frac{-dU_0}{dr} - a_1U(r_0)$. For simplicity, we make a further substitution $\int_{r_0}^r U(\rho)d\rho = I_1$. The first objective function (G_{CM1}) is now constructed as

$$G_{CM1}(a_1, a_2, c_1, \lambda) = \frac{1}{2} \sum_{n=1}^N \left(\frac{dU_n}{dr_n} + a_1U_n + a_2I_{1n} + c_1 \right)^2 + \lambda(2a_1^2 - 9a_2) \longrightarrow \min. \quad (6)$$

Taking partial derivatives, setting the derivatives equal to zero returns a matrix system in three dimensions

$$\begin{bmatrix} a_1(\lambda) \\ a_2(\lambda) \\ c_1(\lambda) \end{bmatrix} = \begin{bmatrix} 4\lambda + \sum_{n=1}^N (U_n)^2 & \sum_{n=1}^N U_n I_{1n} & \sum_{n=1}^N U_n \\ \sum_{n=1}^N U_n I_{1n} & \sum_{n=1}^N (I_{1n})^2 & \sum_{n=1}^N I_{1n} \\ \sum_{n=1}^N U_n & \sum_{n=1}^N I_{1n} & \sum_{n=1}^N 1 \end{bmatrix}^{-1} \times \begin{bmatrix} -\sum_{n=1}^N \left(\frac{dU_n}{dr_n} \right) U_n \\ 9\lambda - \sum_{n=1}^N I_{1n} \left(\frac{dU_n}{dr_n} \right) \\ -\sum_{n=1}^N \left(\frac{dU_n}{dr_n} \right) \end{bmatrix}. \quad (7)$$

The system of Equation (7) is simulated in MathCad[®] to obtain the value of the Lagrange multiplier λ as 0.258 and numerical values for a_1 , a_2 and c_1

$$[a_1(\lambda), a_2(\lambda), c_1(\lambda)]^T = [5.206, 6.022, 0.515]^T. \quad (8)$$

The value of α_1 is estimated using either of the relations $\frac{a_1}{3}$ or $\sqrt{\frac{a_2}{2}}$. This yields $\alpha_1 = 1.735$. The constraint equation is satisfied as $[2a_1(\lambda)]^2 - 9[a_2(\lambda)] = 5.826 \times 10^{-13}$

The second objective function (G_{CM2}) is constructed using Equation (2) as

$$G_{CM2}(\tilde{A}_{CM}, \tilde{B}_{CM}) = \frac{1}{2} \sum_{n=1}^N (\tilde{A}_{CM} e^{-2\alpha_1 r_n} - \tilde{B}_{CM} e^{-\alpha_1 r_n} - U_n)^2 \longrightarrow \min. \quad (9)$$

which reduces to the system

$$\begin{bmatrix} \tilde{A}_{CM}, \tilde{B}_{CM} \end{bmatrix}^T = \begin{bmatrix} \sum_{n=1}^N (e^{-2\alpha_1 r_n})^2 & -\sum_{n=1}^N e^{-3\alpha_1 r_n} \\ -\sum_{n=1}^N e^{-3\alpha_1 r_n} & \sum_{n=1}^N (e^{-\alpha_1 r_n})^2 \end{bmatrix}^{-1} \times \begin{bmatrix} \sum_{n=1}^N U_n e^{-2\alpha_1 r_n}, -\sum_{n=1}^N U_n e^{-\alpha_1 r_n} \end{bmatrix}^T, \quad (10)$$

after partial differentiation with respect to the unknown parameters \tilde{A}_{CM} and \tilde{B}_{CM} and further algebra. Numerical simulation of Equation (10) with $\alpha_1 = 1.735$ and experimental data sets of gold atom [10] yields the following results

$$[\tilde{A}_{CM}, \tilde{B}_{CM}]^T = [4152, 44.679]^T. \quad (11)$$

B. Experimental fitting of data sets to construct potential energy curves

The built-in ‘‘Minimize’’ function in MathCad[®] using estimated parameters of the integral-differential method as initial guess values yielded $\alpha_1 = 1.746$, $\tilde{A}_{CM} = 4739$ and $\tilde{B}_{CM} = 45.886$. Using these approximate values, we

construct the potential energy curves (PECs) in the Figure 1 using Mathematica[®]. U_{Exp}, U_{CM}, U_{CAS} represents the gold atom experimental data sets provided by [10], approximated values obtained using the ObLSf method integral-differential approach and built-in function in MathCad[®] software respectively. The error plots of the reconstructed PECs are graphically illustrated in Figure 2. It should be noted that all potential energy curves were constructed and reconstructed in Mathematica[®] while numerical simulations and calculations were done using MathCad[®].

C. Generalized Morse potential energy function

The Generalized Morse potential considered has a functional form

$$U_{GM} = A_{GM} e^{-\alpha_2 r} - B_{GM} e^{-\alpha_3 r}, \quad (12)$$

which is also a solution of some second-order ODE

$$\frac{d^2 U}{dr^2} + b_1 \frac{dU}{dr} + b_2 U = 0, \quad (13)$$

where $b_1 = \alpha_2 + \alpha_3$ and $b_2 = \alpha_2 \cdot \alpha_3$. The first objective function (G_{GM1}) is formulated by integrating Equation (13) with respect to r .

$$G_{GM1}(b_1, b_2, c_2) = \frac{1}{2} \sum_{n=1}^N \left(\frac{dU_n}{dr_n} + b_1 U_n + b_2 I_{1n} + c_2 \right)^2$$

$$G_{GM1}(b_1, b_2, c_2) \longrightarrow \min, \quad (14)$$

where c_2 (replaces c_1) and I_1 are as defined in Section III-A. The Generalized Morse potential does not need a constraint equation as it has a four parameter space.

We introduce column vectors for U_n, I_{1n} and $\frac{dU_n}{dr_n}$ as $\vec{U} = [U_1, U_2, \dots, U_N]^T, \vec{I} = [I_{1,1}, I_{1,2}, \dots, I_{1,N}]^T, \vec{E} = [1, 1, \dots, 1]^T, d\vec{U} = [dU_1, dU_2, \dots, dU_N]^T$. The short form $d\vec{U}$ represents $\frac{dU_n}{dr_n}$. Equation (14) then reduces to

$$G_{GM1}(b_1, b_2, c_2) = b_1 \vec{U} + b_2 \vec{I} + c_2 \vec{E} + d\vec{U} \longrightarrow \min.$$

$\vec{U}, \vec{I}, \vec{E}$ and $d\vec{U}$ are all $(N \times 1)$ matrices. Partially differentiating this equation with respect to the three unknowns and setting the derivatives to zero, we will obtain

$$[\vec{U} \ \vec{I} \ \vec{E}] \cdot [b_1, b_2, c_2]^T = [-d\vec{U}]. \quad (15)$$

If we represent $[\vec{U} \ \vec{I} \ \vec{E}]$ (an $(N \times 3)$ matrix) as L and $[-d\vec{U}]$ as R , Equation (15) is then simplified using matrix manipulations

$$[b_1, b_2, c_2]^T = (L^T \cdot L)^{-1} \cdot (L^T \cdot R). \quad (16)$$

Numerical simulation of this Equation (16) in MathCad[®] gives the values for b_1, b_2 and c_2

$$[b_1, b_2, c_2]^T = [5.332, 5.853, 0.511]^T. \quad (17)$$

The parameters of the Generalized Morse potential are estimated using the eigenvalues

$$\alpha_2, \alpha_3 = \frac{b_1 \pm \sqrt{b_1^2 - 4b_2}}{2},$$

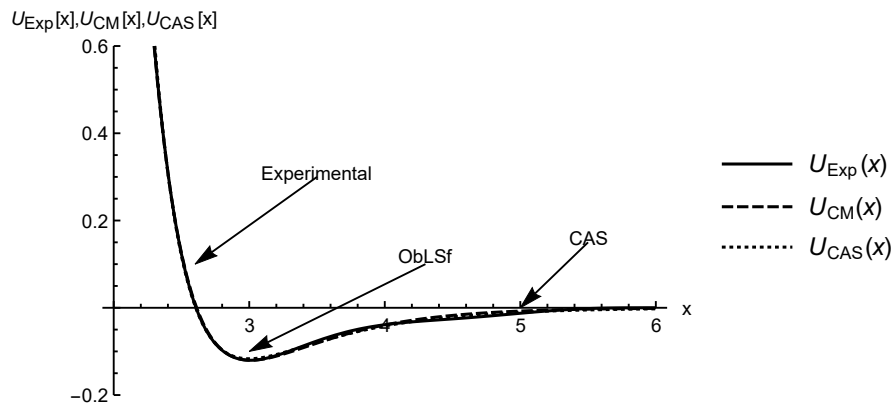


Fig. 1: PECs for estimated Classical Morse potential parameters

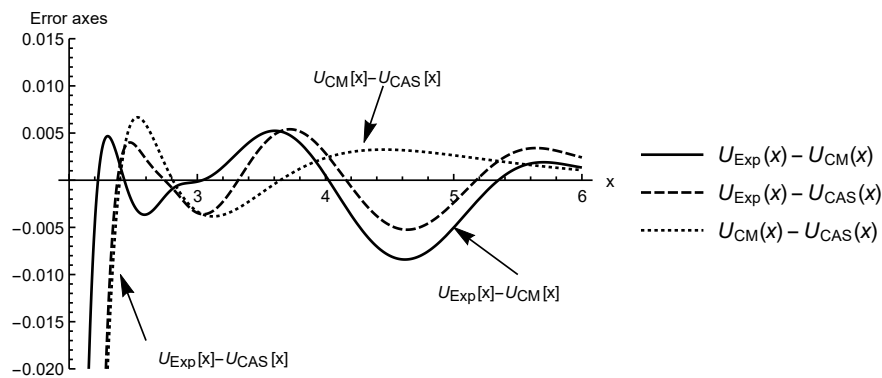


Fig. 2: Error plots of constructed PECs of Classical Morse potential

which yields $\alpha_2 = 3.787$ and $\alpha_3 = 1.546$. The integral-differential approach does not yield complex conjugate eigenvalues at any starting point used to numerically simulate the system in Equation (16). This is in contrast to the ObLSf method and differential approach applied to estimate the parameters of the Classical and Generalized Morse potential in [16] where complex conjugates eigenvalues were obtained for the equivalent α_2 and α_3 parameters. The vector definitions in this section, were introduced to reduce the cumbersome matrix representations. It is also a more computationally efficient approach.

The construction of the second objective function (G_{GM2}) is done using Equation (12) as follows

$$G_{GM2}(\tilde{A}_{GM}, \tilde{B}_{GM}) = \frac{1}{2} \sum_{n=1}^N (\tilde{A}_{GM} e^{-\alpha_2 r_n} - \tilde{B}_{GM} e^{-\alpha_3 r_n} - U_n)^2 \rightarrow \min. \quad (18)$$

Partially differentiating Equation (18) with respect to the unknown parameters \tilde{A}_{GM} , \tilde{B}_{GM} and further simplifying

the resulting equations

$$\begin{bmatrix} \tilde{A}_{GM} \\ \tilde{B}_{GM} \end{bmatrix} = \begin{bmatrix} \sum_{n=1}^N (e^{-\alpha_2 r_n})^2 & -\sum_{n=1}^N e^{(-\alpha_2 + \alpha_3) r_n} \\ -\sum_{n=1}^N e^{(-\alpha_2 + \alpha_3) r_n} & \sum_{n=1}^N (e^{-\alpha_3 r_n})^2 \end{bmatrix}^{-1} \times \begin{bmatrix} \sum_{n=1}^N U_n e^{-\alpha_2 r_n} \\ -\sum_{n=1}^N U_n e^{-\alpha_3 r_n} \end{bmatrix}^T. \quad (19)$$

The numerical simulation of Equation (19) yields

$$[\tilde{A}_{GM}, \tilde{B}_{GM}]^T = [7268, 20.941]^T. \quad (20)$$

D. Experimental fitting of data sets to construct potential energy curves

The built-in “Minimize” function using estimated parameters of the integral-differential approach as initial guess values yielded $\alpha_2 = 3.925$, $\alpha_3 = 1.51$, $\tilde{A}_{GM} = 9681$ and $\tilde{B}_{GM} = 17.784$. The reconstructed PECs as well as their corresponding error plots are presented in Figures 3 and 4. The definitions of U_{Exp} , U_{GM} , U_{CAS} are the same as was defined under Section III-B.

IV. INTEGRAL METHOD FOR ESTIMATION OF THE CLASSICAL MORSE POTENTIAL PARAMETERS

In this section, we consider the second integration of the second-order ODEs examined under Section III-A and III-C, this can also be the integration of the first-order ODEs examined under the sections. In this case, we

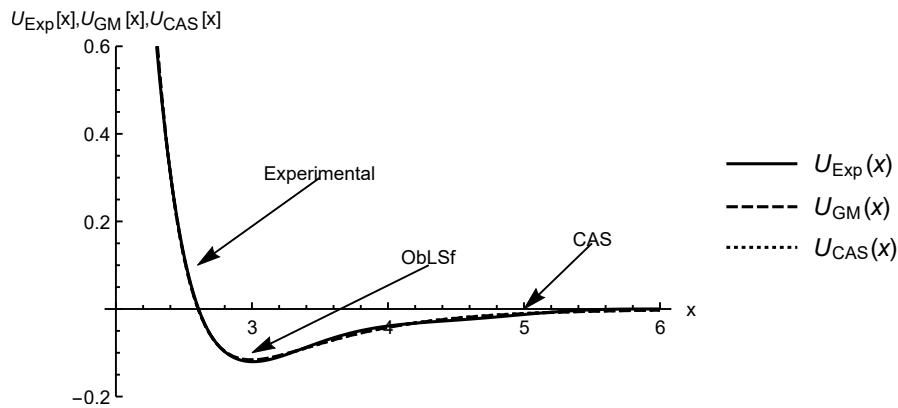


Fig. 3: PECs for estimated Generalized Morse potential parameters

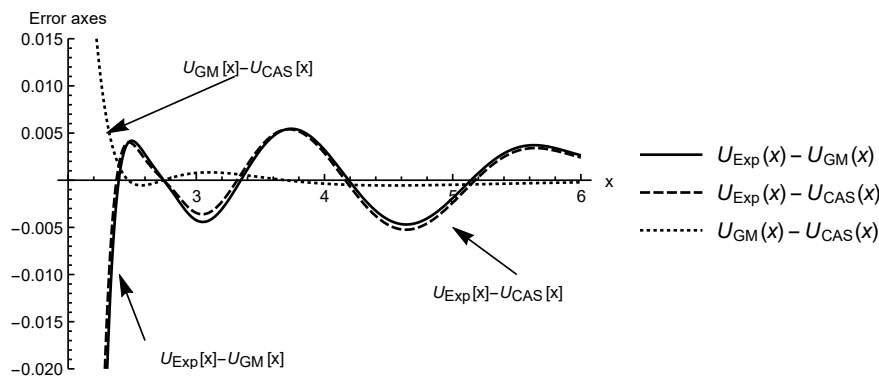


Fig. 4: Error plots of constructed PECs of Generalized Morse potential

don't have any differentials in the first objective functions to be constructed. Hence, no numerical data would be loss due to numerical differentiation of experimental data sets. This is the basis of the supremacy of the numerical integration as compared to the numerical differentiation. The integration of the ODEs is also with respect to r having the boundaries $[r_o, r]$.

A. Classical Morse potential energy function

In this section, we demonstrate the integral approach in estimating parameters of the Classical Morse potential parameters. It involves integrating Equation (4) twice with respect to r within the integral domain $[r_0, r]$ to obtain. Which is in principle, the same as the integration of Equation (5) with respect to r with the domain $[r_0, r]$

$$U(r) + a \int_{r_0}^r U(\rho) d\rho + b \int_{r_0}^r \left[\int_{r_0}^r U(\rho) d\rho \right] d\rho + c\Delta r + d = 0. \tag{21}$$

The substitution $\int_{r_0}^r U(\rho) d\rho = I_1$ and $\int_{r_0}^r \left[\int_{r_0}^r U(\rho) d\rho \right] d\rho = I_2$ is used to make Equation (21) compact, $\Delta r = r - r_0$ and c is equivalent to c_1 in Equation (5). The first objective function (G_{CM1}) used to estimate α_2 is formulated as

$$G_{CM1}(a, b, c, d, \lambda) = \frac{1}{2} \sum_{n=1}^N \{U(r) + aI_{1n} + bI_{2n} + c\Delta r + d\}^2 + \lambda(2a^2 - 9b) \rightarrow \min. \tag{22}$$

Here the constraint equation of the Classical Morse potential is $g[a(\lambda), b(\lambda)] = [2a(\lambda)]^2 - 9[b(\lambda)]$. Differentiating Equation (22) partially with respect to the four unknown parameters (a, b, c, d) yields a matrix in 4 dimensions

$$[a(\lambda), b(\lambda), c(\lambda), d(\lambda)]^T = \begin{bmatrix} 4\lambda + \sum_{n=1}^N (I_{1n})^2 & \sum_{n=1}^N I_{2n} I_{1n} & \sum_{n=1}^N I_{1n} \Delta r_n & \sum_{n=1}^N I_{1n} \\ \sum_{n=1}^N I_{1n} I_{2n} & \sum_{n=1}^N (I_{2n})^2 & \sum_{n=1}^N I_{2n} \Delta r_n & \sum_{n=1}^N I_{2n} \\ \sum_{n=1}^N I_{1n} \Delta r_n & \sum_{n=1}^N I_{2n} \Delta r_n & \sum_{n=1}^N (\Delta r_n)^2 & \sum_{n=1}^N \Delta r_n \\ \sum_{n=1}^N I_{1n} & \sum_{n=1}^N I_{2n} & \sum_{n=1}^N \Delta r_n & \sum_{n=1}^N 1 \end{bmatrix}^{-1} \times \begin{bmatrix} -\sum_{n=1}^N U_n I_{1n} \\ 9\lambda - \sum_{n=1}^N U_n I_{2n} \\ -\sum_{n=1}^N U_n \Delta r_n \\ -\sum_{n=1}^N U_n \end{bmatrix}. \tag{23}$$

The numerical simulation yields value of the Lagrange multiplier, $\lambda = -0.611$ and Equation (23) as

$$[a(\lambda), b(\lambda), c(\lambda), d(\lambda)]^T = [-0.685, 0.104, -0.023, 0.536]^T. \quad (24)$$

This gives $\alpha_1 = 0.228$. The values of a and b satisfies the constraint equation.

The second objective function (G_{CM2}) is the same as Equation (9) and the matrix system to be obtained is same as in Equation (10), α_1 will only be replaced by α_2 . Numerical simulation yields results of the values of \tilde{A}_{CM} and \tilde{B}_{CM}

$$[\tilde{A}_{CM}, \tilde{B}_{CM}]^T = [0.552, 0.297]^T. \quad (25)$$

It is clearly observable from the numerically simulated values α_1, \tilde{A}_{CM} and \tilde{B}_{CM} of the Classical Morse potential, that the integral method fails to give estimates that converge to the optimal solution. The authors in [16] discovered that the built-in ‘‘Minimize’’ (Levenberg-Marquardt) algorithm embedded in Mathematica[®] failed to minimize the Classical Morse potential as the estimated parameter values did not have a global minimum. This can be due to the nonuniqueness of the Classical Morse potential functional form.

Using these values that fail to converge to the optimum solution as initial guess values (IGVs) in the built-in ‘‘Minimize’’ algorithm returns the values $\alpha_1 = 1.746, \tilde{A}_{CM} = 4379$ and $\tilde{B}_{CM} = 45.886$ and the corresponding optimized value is shown in Table I. The reconstructed PECs for the Classical Morse potential parameters is shown in Figure 5. As can be seen, the approximations using the estimates that failed to converge to the optimum solutions as IGVs in the built-in algorithm of MathCad[®] are good.

B. Generalized Morse potential energy function

The integral approach yields the equation (see Equation (22)) as obtained in Section IV-A, we only use different notations for the first objective function (G_{GM1}) to estimate the parameters α_2 and α_3 .

$$G_{GM1}(e, f, g, h) = \frac{1}{2} \sum_{n=1}^N \{U(r) + eI_{1n} + fI_{2n} + g\Delta r + h\}^2$$

$$G_{GM1}(e, f, g, h) \longrightarrow \min. \quad (26)$$

This is because the second-order ODE are similar and the second integration yields the same equation. In this section, we also introduce column vectors as was done previously for the integral-differential section. The following definitions apply, $\vec{I}_1 = [I_{1,1}, I_{1,2}, \dots, I_{1,N}]^T, \vec{I}_2 = [I_{2,1}, I_{2,2}, \dots, I_{2,N}]^T, \vec{\Delta r} = [\Delta r_1, \Delta r_2, \dots, \Delta r_N]^T, \vec{E}_1 = [1, 1, \dots, 1]^T$ and $\vec{U} = [U_1, U_2, \dots, U_N]^T$ where \vec{U} represents $U(r)$. This definitions reduces the objective function in Equation (26)

$$G_{GM1}(e, f, g, h) = \vec{U} + e\vec{I}_1 + f\vec{I}_2 + g\vec{\Delta r} + h\vec{E}_1 \longrightarrow \min.$$

We partially differentiate this equation with respect to the four unknowns and after some algebra

$$[\vec{I}_1 \ \vec{I}_2 \ \vec{\Delta r} \ \vec{E}_1] \cdot [e, f, g, h]^T = -[\vec{U}]. \quad (27)$$

The notation $L = [\vec{I}_1 \ \vec{I}_2 \ \vec{\Delta r} \ \vec{E}_1]$ (an $N \times 4$ matrix) and $R = -[\vec{U}]$ (an $(N \times 1)$ matrix) is used to simplify Equation (27)

$$[e, f, g, h]^T = (L^T \cdot L)^{-1} \cdot (L^T \cdot R), \quad (28)$$

which is numerically simulated to yield the values

$$[e, f, g, h]^T = [5.592, 5.856, 0.522, -0.013]^T. \quad (29)$$

The relation

$$\alpha_2, \alpha_3 = \frac{e \pm \sqrt{e^2 - 4f}}{2},$$

gives $\alpha_2 = 4.196$ and $\alpha_3 = 1.395$.

The second objective function (G_{GM2}) is the same as in Equation (18) while the corresponding matrix system to be obtained is same as Equation (19), where α_2 and α_3 replaces α_2 and α_3 . Numerical simulations of Equation (19) for this section yields

$$[\tilde{A}_{GM}, \tilde{B}_{GM}]^T = [16780, 11.386]^T. \quad (30)$$

C. Experimental fitting of data sets to construct potential energy curves

The reconstructed PECs of the integral approach for this section and the corresponding error plots are presented in Figures 6 and 7.

V. A NOVEL APPROACH

In this paper, we have identified the Classical and Generalized Morse potentials using the Objective least squares function, ObLSf, method with the integral-differential and integral approaches. We refer to this method as the Lagrange multiplier method. The aforementioned method is based on reliable methods readily available in literature and it was well-detailed in the estimation of the energy potential parameters. We concisely demonstrate a more comprehensive evaluation of this paper by proposing a novel approach. Considering Equation (4), replacing a_1, a_2 by C_1, C_2 and integrating the equation twice with respect to r within the domain $[r_0, r]$

$$U(r) + C_1 I_1(r) + C_2 I_2(r) + C_3 + C_4 \Delta r = 0, \quad (31)$$

where the definitions $C_4 = -(U'_0 + C_1 U_0), C_3 = -U_0$ apply and $I_1(r), I_2(r)$ retain their previous definitions. The Equation (31) linearly depends on C_1, \dots, C_4 unknown parameters and there is one constraint between C_1 and C_2 parameters

$$2C_1^2(C_4) - 9C_2(C_4) = 0. \quad (32)$$

We introduce the parameters C_3 and C_4 to account for statistical uncertainty of experimental data sets. Let us consider C_4 as a variable parameter so that C_1, \dots, C_3 coefficients are considered as functions of this auxiliary parameter: $C_1 = C_1(C_4), C_2 = C_2(C_4), C_3 = C_3(C_4)$. The objective function is now constructed as

$$G(C_1, C_2, C_3, C_4) = \frac{1}{2} \sum_{i=1}^N [C_1 I_{1i} + C_2 I_{2i} + C_3 + (U_i + C_4 \Delta r_i)]^2 \longrightarrow \min. \quad (33)$$

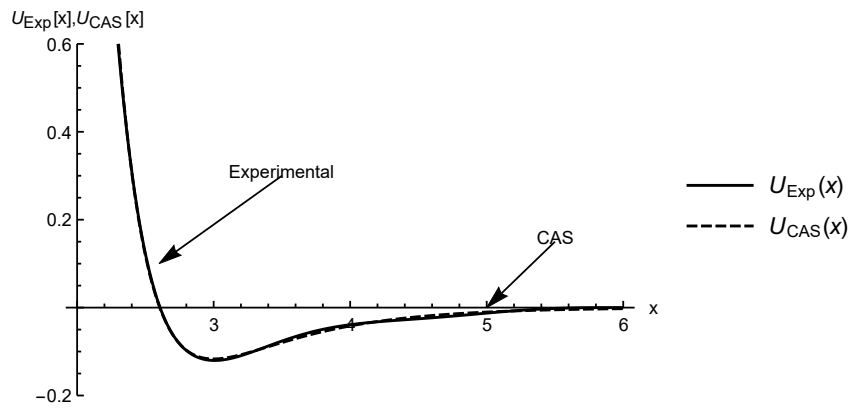


Fig. 5: PECs for estimated Classical Morse potential parameters

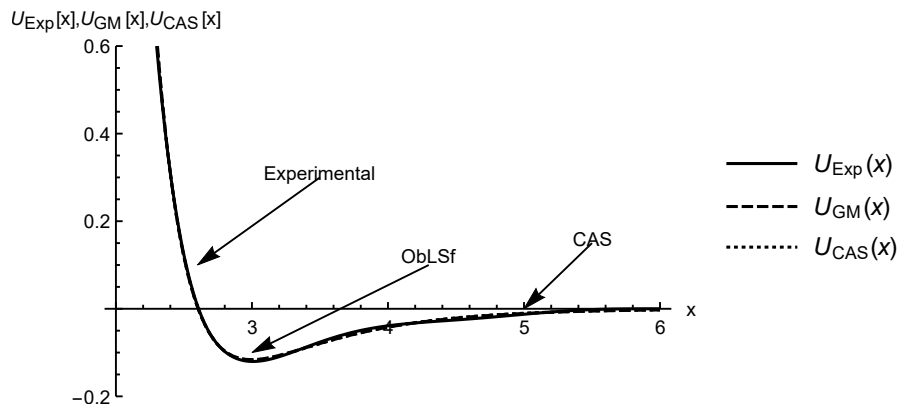


Fig. 6: PECs for estimated Generalized Morse potential parameters

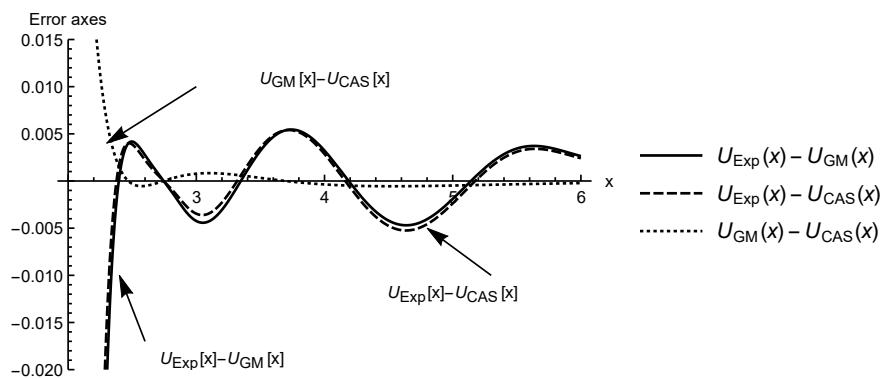


Fig. 7: Error plots of constructed PECs of Generalized Morse potential

Next, we partially differentiate the objective function with respect to all three parameters C_1, \dots, C_3 , equalize them

to zero and obtain the system whose solution is

$$\begin{aligned}
 \begin{bmatrix} C_1(C_4) \\ C_2(C_4) \\ C_3(C_4) \end{bmatrix} &= \begin{bmatrix} \sum_{i=1}^N (I_{1i})^2 & \sum_{i=1}^N I_{1i}I_{2i} & \sum_{i=1}^N I_{1i} \\ \sum_{i=1}^N I_{2i}I_{1i} & \sum_{i=1}^N (I_{2i})^2 & \sum_{i=1}^N I_{2i} \\ \sum_{i=1}^N I_{1i} & \sum_{i=1}^N I_{2i} & \sum_{i=1}^N 1 \end{bmatrix}^{-1} \\
 &\times \left\{ \begin{bmatrix} -\sum_{i=1}^N I_{1i}U_i & -\sum_{i=1}^N I_{1i}I_{2i} & -\sum_{i=1}^N U_i \end{bmatrix}^T \right. \\
 &\left. + C_4 \cdot \begin{bmatrix} \sum_{i=1}^N I_{1i}\Delta r_i & \sum_{i=1}^N I_{2i}\Delta r_i & \sum_{i=1}^N \Delta r_i \end{bmatrix}^T \right\}. \tag{34}
 \end{aligned}$$

Next, we solve $2C_1^2(C_4) - 9C_2(C_4) = 0$ to obtain C_4 . The numerical simulation of the system in Equation (34) practically gives the same results as those generated using the Lagrange multiplier method detailed in this paper. The advantage of this novel approach is that we calculated the coefficient matrix only once but the coefficient matrix is calculated for every λ using the Lagrange multiplier method. This means, if there are 1000λ parameters, the coefficient matrix would be calculated for every single λ . The novel approach can also be applied to any equation regardless of how complex the constraint equation(s) is(are). The Lagrange multiplier method, on the other hand, cannot be applied to equations having complex constraint equations (i.e. it can only be applied to equations having a quadratic constraint equation). This is further expatiated by considering the Classical Rydberg potential and Generalized Rydberg potential energy functions

$$U^{CR}(r) = (A_1 + A_2r)e^{-\alpha r}, \quad (35)$$

$$U^{GR}(r) = (A_1 + A_2r + A_3r^2)e^{-\alpha r}. \quad (36)$$

Equation (35) has the characteristic equation $(\lambda + \alpha)^2$ and constraint $C_1^2 - 4C_2 = 0$ while Equation (36) has the characteristic equation $(\lambda + \alpha)^3$ and constraints $C_1^2 - 3C_2 = 0, C_1C_2 - 9C_3 = 0$ and $C_1^3 - 27C_3 = 0$. In the case of the Generalized Rydberg energy potential, the Lagrange multiplier method cannot be used due to the cubic constraint equation. The method can not be used in cases where the constraint equation(s) is nonlinear. Although, the Classical Rydberg and Generalized Rydberg potentials are not the focus of this paper, we only use their analytic forms to expatiate on how the novel approach (in comparison with the Lagrange multiplier method) is more applicable to problems having more complex constraints. A brief look at the dimensions of the matrices in Equations (23) and (34) also shows the superiority of the Novel approach to the Lagrange multiplier method. The Novel approach will be well-detailed in identifying energy potentials such as Classical Rydberg, Generalized Rydberg, Generalized Morse, Simplified Buckingham and Extended-Rydberg potentials in future investigations.

VI. RESULTS AND DISCUSSION

The approaches that we considered in this work are more accurate than the ObLSf method and differential approach used in [16], they were used to estimate parameters of hybrid functional forms of the Morse potential. Figure 6 shows the very good approximations of the integral approach as the reconstructed PECs for the experimental data sets of gold atom, estimated parameters using the integral approach and built-in function in MathCad[®] are almost graphically indistinguishable. The errors in Figure 7 are also very small. Table I shows that the integral approach gives better approximations compared to the integral-differential approach (and even the ObLSf method and differential approach in [16]). The integral approach is therefore a preferred approach for estimation of potentials as it filters random perturbation and prevents numerical loss of data. It should be noted that the optimized goal function value for the Classical Morse

potential in Table I was obtained using the estimated values that did not converge to the optimal solution as IGVs for the built-in algorithm in MathCad[®]. Table II compares the estimated Morse potential parameters obtained using the integral-differential approach presented in this work with estimated parameters in the literature for gold (Au-Au), aluminum (Al-Al), chromium (Cr-Cr) and iron (Fe-Fe) metal atoms. The disparities observed between the values of D(eV) in our approach and the existing values in literature is due to the fact that different experimental data sets were used in obtaining the results. The disparities between the values of $r_m(A^0), \alpha(1/A^0)$ in our approach and existing values are reasonably acceptable.

Figure 5 illustrates that although the integral approach fails for the Classical Morse potential energy function, the obtained values can be used as starting IGVs with the “Minimize” algorithm in MathCad[®] to obtain quite good approximations when fitted to experimental data sets of gold atom [10].

VII. CONCLUSION

In this paper, we estimated the parameters of the Classical and Generalized Morse potential using the (relatively) more accurate integral-differential and integral approaches. These approaches are more accurate because they filter random perturbation as opposed to differential approach which causes numerical loss of data. In [16], the built-in “Minimize” function failed to produce estimates that converge to the optimum solution. In this paper, the integral approach failed to estimate parameters of the Classical Morse potential using the ObLSf method and integral approach. This paper therefore validates that, the Generalized Morse potential is a more viable hybrid form of the Morse potential. We further confirm this proposition by papering the values presented in Table I. The closer the values are to 1, the less accurate the approximated estimates, the farther the values are from 1, the more accurate the approximated estimates. From this standpoint, the initial proposition is validated. This paper also shows that the approaches applied, gives good estimates that agrees with experimental data sets of gold atom globally and locally, within the whole range of interatomic distance. A novel approach was concisely introduced and comparisons were made between both methods outlined in this paper.

ACKNOWLEDGMENT

The authors wishes to acknowledge the Department of Mathematics and Statistics and the Department of Higher Education and Training for funding this research.

REFERENCES

- [1] T. Barakat, K. Abodayeh, and O. Al-Dossary, Exact solutions for vibrational levels of the Morse potential via the asymptotic iteration method, *Czechoslovak Journal of Physics*, vol. 56, no. 6, pp. 583-590, 2006.
- [2] L. A. Girifalco and V. G. Weizer, Application of the Morse potential function to cubic metals, *Physical Review*, vol. 114, no. 3, pp. 687, 1959.

TABLE I: Values of Goal function for estimated potential parameters for the integral-differential and integral approach

Method	Integral-differential approach	Integral approach
Classical Morse potential	0.051	0.05
Generalized Morse potential	0.036	0.034

[3] C. R. Kikawa, T. N. Malange, M. Y. Shatalov, and S. V. Joubert, Identification of the Rydberg interatomic potential for problems of nanotechnology. *Journal of Computational and Theoretical Nanoscience*, vol. 13, no. 7, pp. 4649-4655, 2016.

[4] I. G. Kaplan, Intermolecular interactions: Physical picture, Computational methods and Model potentials, *John Wiley & Sons*, 2006.

[5] A. C. P. Mkolesia, Parameter Estimation methods for different Probability Density Functions, *Ph.D. thesis*, Tshwane University of Technology, 2017.

[6] T. N. Malange, Alternative parameter estimation methods of the classical Rydberg interatomic potential, *Master's thesis*, Tshwane University of Technology, 2016.

[7] P. M. Morse, Diatomic molecules according to the wave mechanics. II. Vibrational levels, *Physical Review*, vol. 34, no. 1, pp. 57, 1929.

[8] K. Madsen, H. B. Nielsen and O. Tingleff, Methods for non-linear least squares problems, *Technical Report, Informatics and Mathematical Modelling*, Technical University of Denmark, 2004.

[9] M. Ngungu, C. R. Kikawa, A. C. Mkolesia, and M. Y. Shatalov, Parameter identification for the Gumel-Mickens HIV transmission model under missing observable data. *Global Journal of Pure and Applied Mathematics*, vol. 13, no. 11, pp. 7759-7770, 2017.

[10] P. A. Olsson, Transverse resonant properties of strained gold nanowires, *Journal of Applied Physics*, vol. 108, no. 3, pp. 034318, 2010.

[11] P. G. Hajigeorgiou, An extended Lennard-Jones potential energy function for diatomic molecules: Application to ground electronic states, *Journal of Molecular Spectroscopy*, vol. 263, pp. 101 – 110, 2010.

[12] H. Pamuk and T. Halicioğlu, Evaluation of Morse parameters for metals, *Physica Status Solidi (a)*, vol. 37, no. 2, pp. 695-699, 1976.

[13] R. Lincoln, K. Koliwad, and P. Ghate, Morse-potential evaluation of second-and third-order elastic constants of some cubic metals. *Physical Review*, vol. 157, no. 3, pp. 463, 1967.

[14] A. C. Mkolesia, C. R. Kikawa, and M. Y. Shatalov, Estimation of the Rayleigh distribution parameter. *Transylvanian Review*, vol. 24, no. 8, 2016.

[15] M. Reith, Nano-engineering in Science and Technology: an Introduction to the World of Nano-design. *World Scientific*, 2003.

[16] S. A. Surulere, M. Y. Shatalov, A. C. Mkolesia, and I. A. Fedotov, A modern approach for the identification of the Classical and Modified Generalized Morse potential, *Nanoscience & Nanotechnology - Asia*, Accepted for publication, 2019.

	Our method		Ref. [2]		Ref. [13]		Ref. [12]		
	D (eV)	$r_m(A^0)$	$\alpha(1/A^0)$	D (eV)	$r_m(A^0)$	$\alpha(1/A^0)$	D (eV)	$r_m(A^0)$	$\alpha(1/A^0)$
Au-Au	0.12	3.011	1.735	0.4753	3.0242	1.5830	0.49005	2.99032	1.66136
Al-Al	0.123	3.178	1.089	0.2700	3.4068	1.0341	0.29614	3.29692	1.11892
Cr-Cr	0.462	3.116	1.116	0.4414			0.45247	2.78451	1.50992
Fe-Fe	0.028	3.636	1.357	0.4174			0.43609	2.83152	1.40262

TABLE II: Comparison of estimated Morse potential parameters with existing results in the literature